J Mater Sci (2006) 41:6897–6907
DOI 10.1007/s10853-006-0222-5

Materials selection for thermal comfort in passive solar buildings

J. M. Thomas · S. Algohary · F. Hammad · W. O. Soboyejo

Received: 30 September 2004 / Accepted: 29 September 2005 / Published online: 7 October 2006

Abstract This paper presents the results of a combined analytical, computational, and experimental study of the key parameters for selecting affordable materials and designing for thermal comfort in passive solar buildings. The heat transfer across the walls of buildings is modeled using a simple heat diffusion model. In this way, the passive heat storage from the sun (passive solar) and the heat load from internal heat sources are stored in the walls of buildings that provide internal cooling during the day and internal heating at night. The simple analytical model of heat diffusion is used to identify the merit indices for the optimization of affordable passive solar performance. The time dependence of wall/internal temperature is then simulated using a simple finite difference model. The results from the analytical model and finite difference model are validated by conducting temperature measurements in two affordable housing complexes in Egypt. The implications of the results are then discussed for the design of thermal comfort in affordable housing.

Introduction

The artisans of ancient Egypt developed buildings that provided passive solar heating or cooling by the creative use of architecture and materials science and engineering [1]. Although much of the knowledge that they developed has been lost with time, a number of Egyptian architects have made strong efforts to recreate the dome buildings that provided the thermal comfort in ancient Egypt [2]. Prominent among these was the Egyptian architect, Hassan Fathy, who pioneered ''new'' architecture for the poor in the last century [1]. Since then, the disciples of Hassan Fathy have built residential dwellings and art galleries that utilize the knowledge of ancient Egypt [1]. These buildings include the Egyptian Atomic Energy Authority's Inshas guesthouse and the Wissa Wassef Art Centre, both located near Cairo.

Although the internal temperatures in these buildings are often comparable for those in air-conditioned buildings [3, 4], the authors are unaware of prior efforts to apply heat transfer concepts to the design of affordable passive solar buildings that use their walls and ceilings as heat sinks and sources (Fig. 1). Such heat transfer concepts, which were developed long after the empirical and creative advances of ancient Egypt, may provide the basis for the application of passive solar concepts on a more global scale.

With the increasing cost of energy, it is clear that ongoing building practices that depend almost entirely on active heating and cooling cannot be sustained indefinitely [1–5]. There is, therefore, a need to consider alternative approaches to the internal heating or cooling that is required to provide thermal comfort in buildings. Please note that thermal comfort in this paper refers specifically to the inner air temperature. However, it is recognized that a more general definition of thermal comfort could include consideration of other factors such as relative humidity.

This paper presents one alternative approach to the selection of affordable building materials that provide internal heating and cooling throughout the day. Following the introduction, a theoretical framework is presented for the selection of affordable materials that enable well-controlled internal heating or cooling by heat diffusion into

J. M. Thomas · W. O. Soboyejo (✉)
Department of Mechanical and Aerospace Engineering,
Princeton University, Princeton, NJ 08544, USA
e-mail: soboyejo@princeton.edu

S. Algohary · F. Hammad
Egyptian Atomic Energy Authority, Cairo, Egypt

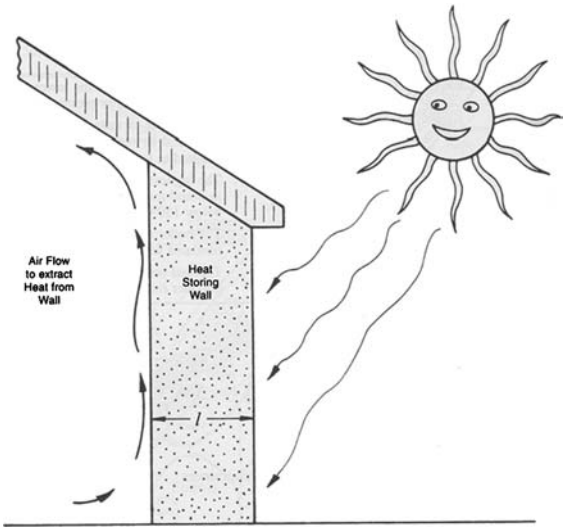

Fig. 1 The passive solar concept uses walls for heat storage

the walls or roofs of buildings. The possible wall temperature and internal temperature variations are then simulated within a finite difference model. The predicted temperature variations are shown to be consistent with experimental measurements from two Egyptian housing complexes that utilize passive solar concepts in the design. The implications of the results are then discussed for the selection of affordable materials for passive solar buildings.

Theoretical model and computer simulation

Design objectives and constraints

When designing a building it is important to integrate architecture and material choice in order to encourage optimal performance of the structure. Of particular interest is the control of interior temperature and costs associated with construction and operation of the facility. To provide thermal comfort, a reasonable internal temperature must be maintained—both in mean value and oscillation amplitude. Additionally, the time lag between interior and exterior heat fluxes and temperatures must be controlled. Finally, the design must consider the immediate and life cycle cost associated with a given material.

Temperature profile

The temperature profile within a building is influenced by many factors, including material selection and architecture [3, 4]. To characterize the interior temperature profile with respect to that of the exterior, three independent parameters must be defined: mean shift, decrement factor, and time lag. The mean shift (θ) defines the difference between the interior air and exterior surface mean temperatures; the decrement factor (μ) is the ratio of interior and exterior amplitude; and the time lag (ϕ) is the phase shift between the exterior and interior temperature profiles. These three parameters are related through the material selection and architecture; a desirable temperature profile can be achieved by choosing proper materials and architectural schemes.

Any wall, regardless of thickness and material choice, will cause a reduction in the temperature amplitude. This reduction ratio (inside amplitude to outside amplitude), is a function of wall thickness, material properties, and the driving frequency [3, 6]:

$$\mu = \exp(-l\sqrt{\frac{\omega\rho c}{2k}}), \tag{1}$$

where ω is the driving frequency, ρ is the density, c is the specific heat, and k is the thermal conductivity. Defining thermal diffusivity, α, as ($\alpha = \frac{\rho c}{k}$), the decrement factor becomes:

$$\mu = \exp(-l\sqrt{\frac{\omega}{2\alpha}}). \tag{2}$$

For a one-day cycle, the driving frequency is assumed to be constant and has a value of:

$$\omega = \frac{2\pi}{24 * 3600}. \tag{3}$$

The time lag is also a function of wall thickness, thermal diffusivity, and driving frequency [3]:

$$\phi = l\sqrt{\frac{1}{2\omega\alpha}}. \tag{4}$$

The third parameter of interest is the mean temperature shift across the wall. If there is a net heat flux through a wall during a day, there will be a shift in the mean temperature within the room. If heat is removed from the room on a net basis, the mean room temperature will be below that of the exterior, and vice versa. Figure 2 illustrates the thermal gradients that cause heat flow into the wall from the outside environment.

The net heat flux can be the result of air conditioners (in the case of cooling) or lights, computers, appliances, or humans (in the case of heating). Other walls, the floor, and the ceiling may also provide or remove a net amount of heat during a day. The ratio of the temperature shift to the net heat flux through the wall is defined as the thermal resistance of the system (comprising the wall and interior air mass):

$$R = \frac{T_{\text{in}} - T_{\text{out}}}{Q_{\text{net}}} = \frac{\theta}{Q_{\text{net}}}. \tag{5}$$

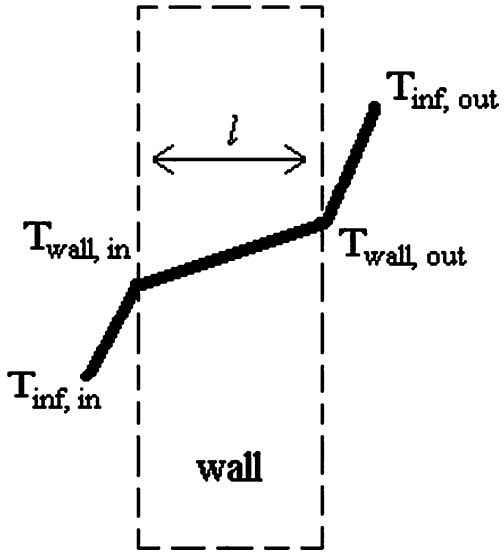

Fig. 2 Thermal gradient across wall and convective boundary layers

The total resistance, R, is the sum of the thermal resistances seen across the wall and the air.

$$R = R_{\text{wall}} + R_{\text{air}}. \tag{6}$$

The thermal resistance of the wall is inherently linked to the thickness, l, and thermal conductivity, k, of the wall:

$$R_{\text{wall}} = \frac{l}{k}. \tag{7}$$

Written differently, the thermal resistance becomes:

$$R_{\text{wall}} = \frac{l}{\alpha\rho c}. \tag{8}$$

The thermal resistance between the wall's inner surface and the interior air is given by

$$R_{\text{air}} = \frac{1}{h}, \tag{9}$$

where h is the convection coefficient on the wall's interior surface. Therefore, the ratio of mean shift to heat flux can be written as:

$$\frac{T_{\text{in}} - T_{\text{out}}}{Q_{\text{net}}} = \frac{l}{k} + \frac{1}{h}. \tag{10}$$

For the case of natural convection occurring on the interior surface of the wall, the convection coefficient is quite small and therefore presents a large thermal resistance. For simplicity, the convection coefficient shall be assumed to be equal to two (R_{air}=0.5), which is a typical value under these circumstances. With this simplification, the total thermal resistance becomes only a function of wall thickness and conductivity. Note that this neglects convection of the outer walls, ceilings and floors. This is done for the sake of simplicity in the current one-dimensional model.

It can be seen that the three temperature parameters (thermal resistance, decrement factor, and time lag) are all functions of diffusivity and wall thickness. Additionally, the mean shift depends on the volumetric heat capacity. The importance of this functional similarity is that for a given wall thickness, these parameters can be displayed on a single graph, shown in Fig. 3. For a certain wall thickness, the diffusivity is dictated by the desired decrement factor or time lag. At this diffusivity, a number of thermal resistances exist (corresponding to a unique thermal conductivity, based on the wall thickness—see Eq. 7). The material selection is made by choosing an appropriate thermal resistance that will provide the desired mean shift at a given net heat flux. Of course, the design process could be executed in the reverse order: specifying a resistance and material will dictate the necessary wall thickness to achieve a given time lag or decrement factor.

Thermal resistance as a design tool

When designing a passive solar structure, all components of the building must function together to achieve the desired result; all components must be designed to perform in a certain manner. For example, if a simple four-walled building is being designed (Fig. 4), the thermal contribution of the floor, ceiling, and walls must each be considered. If the average interior temperature is to be below that of the exterior, then heat must be removed from inside the room on a net basis. The net heat gain inside the building must be zero if the structure is in equilibrium:

$$Q_{\text{north}} + Q_{\text{south}} + Q_{\text{east}} + Q_{\text{west}} + Q_{\text{floor}} + Q_{\text{ceiling}} + Q_{\text{other}} = 0. \tag{11}$$

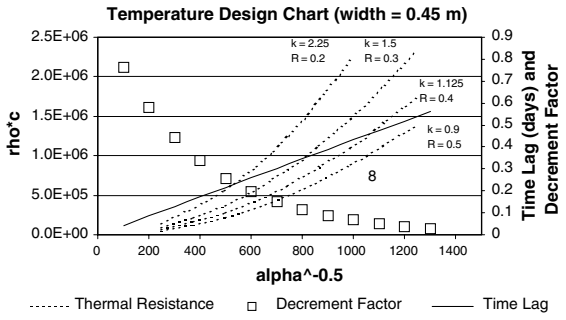

Fig. 3 Graphical relationship between time lag, amplitude gain, and thermal resistance

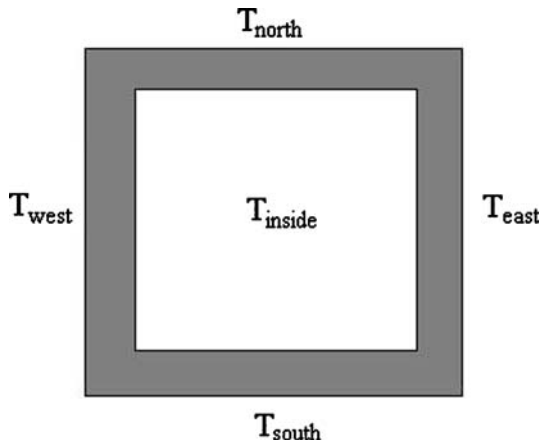

Fig. 4 Schematic of building with four walls

Given a desired interior temperature and an exterior surface temperature (based on the orientation) and thermal resistance for each wall, it is possible to calculate the amount of heat that must be removed from the room—either through the ceiling and floor or by other mechanisms (such as ventilation).

$$Q_{\text{floor}}+Q_{\text{ceiling}}+Q_{\text{other}}=-\sum_i \frac{\Delta T_i}{R_i}. \tag{12}$$

In the above equation, a summation is made of all the temperature differences (inside to outside) for the structure: north, south, east, and west. This relationship is very useful in the architectural design of the building, particularly when selecting ceiling geometry and ventilation mechanisms.

Heat transfer model

The analysis assumes a vertical flat plate in which natural convection dominates heat transfer. The heat flux into the wall from inside a room is defined as:

$$Q = h(T_{\text{air}} - T_{\text{wall}}), \tag{13}$$

where h is the convective heat transfer coefficient between the wall and air [2].

The observed temperature profile for the air mass inside the room can be used to determine the amount of heat entering the room throughout the day. By noting the change in temperature each hour, it is possible to infer the heat flow during that hour. The relationship between heat flow and temperature change is given to be:

$$Q_{\text{room}} = \rho_{\text{air}} V c_{\text{air}} \frac{\mathrm{d}}{\mathrm{d}t}(T_{\text{air\_inside}}), \tag{14}$$

where V is the volume of air within the room.

Computer simulation

A finite difference model was used to simulate the heat transfer occurring within the wall and at the boundaries. The model is based on the simple one-dimensional heat diffusion equation:

$$\alpha \frac{\partial^2 T}{\partial x^2} = \frac{\partial T}{\partial t}. \tag{15}$$

The above equation is discretized through a central differencing scheme, with the interior wall surface taken to be at $x = 0$. The time-stepped nodal equations within the wall become:

$$T_i^{n+1} = \frac{\alpha \Delta t}{\Delta x^2}(T_{i+1}^n - 2T_i^n + T_{i-1}^n) + T_i^n, \tag{16}$$

where the subscript i represents a special increment and the superscript n indicates the time step. A correct definition of the boundary conditions is crucial to the accuracy of the simulation. On the wall's exterior surface, convective and radiative heat transfer is present. Solar radiation warms the surface during the day, and heat is lost to space and the surrounding environment at night. The radiative gain or loss, Q_{rad} is input into the simulation as a function of time. The convective heat transfer is a highly dependent on the convection coefficient, h_outer, which is the result of both forced and natural convection on the outer surface.

$$T_{i\_\text{outer}}^{n+1} = \frac{k}{k + h\Delta x}\left(T_{i\_\text{outer}-1}^{n+1} + \frac{h\Delta x}{k} T_{\text{air\_outside}} + Q_{\text{rad}} \frac{\Delta x}{k}\right). \tag{17}$$

On the interior surface, heat is transported through natural convection.

$$T_1^{n+1} = \frac{h\Delta x}{k + h\Delta x}\left(T_{\text{air\_inside}} + \frac{k}{h\Delta x} T_2^n\right). \tag{18}$$

At each time step, the interior air temperature is calculated, based on the amount of heat entering the room through the wall and from other sources; a variable internal heat load, Q_{inside} (positive or negative), is included as a variable to replicate the presence of other heat sources or sinks.

$$T_{\text{air\_inside}}^{n+1} = \frac{\Delta t}{\rho_{\text{air}} c_{\text{air}} V}\left(Q_{\text{inside}} + \frac{k}{A}\left.\frac{\mathrm{d}T}{\mathrm{d}x}\right|_{x=0}\right) + T_{\text{air\_inside}}^n, \tag{19}$$

where 'A' is the surface area of the wall.

Cost model

The material selection process must include an investigation of cost. Although the true cost of using a material varies by location (the material may be indigenous to the area or the construction costs may be dependant highly on the material, for example), a simplified model is presented here in which the cost is determined by an average bulk material cost. A material's cost, per unit area, is given by:

$$\text{Cost} = l\rho c_m, \tag{20}$$

where c_m is the cost per unit mass. A relationship between cost and diffusivity for maximal heat storage in a wall is given by Ashby, [5], as:

$$\text{Cost} = \frac{\alpha^{1/2}\rho c_m}{\sqrt{w}}. \tag{21}$$

In order to minimize cost, the quantity $\alpha^{1/2}\rho c_m$ must be minimized; this becomes the merit index for cost. Because the driving frequency of the exterior heat load is not variable (see Sect. ''Temperature profile''), the cost becomes a function only of material properties.

It is important to note here that this simple materials cost neglects life cycle costs and the savings on heating and ventilation costs that must be balanced against the additional cost of the increased thermal mass. Hence, the simple model presented here is intended only for materials selection and design within the simplified context presented by Ashby. Further work is clearly needed to establish a more comprehensive framework that could include heating and ventilation costs, and comparative analyses of the additional cost of thermal mass. These are beyond the scope of the current work.

Experimenal procedure

Three rooms at the Inshas Science City Project Guest House were selected for thermal observation (see Ref. [2] and Appendix A for a description of the Inshas facility and a plan of the building). The first room—a bedroom on the northern side of the building—has a high domed ceiling. In contrast, the second room faces south and has a vaulted ceiling. Finally, the third room is on the northwest corner of the building and has a shallow dome as a ceiling. Both the first and second rooms are on the ground floor, while the third is on the first floor.

All windows and doors in the three rooms were closed, and all attempts were made to maintain a constant air mass within the rooms. The temperature measurements were made after periods of similar temperature variations. Beginning at 11:30 a.m. on July 31, 2004, hourly air and wall temperature measurements—interior and exterior air and wall temperatures—were taken for each room (north room beginning at 11:30 a.m., south room beginning at 11:50 a.m., and northwest beginning at 12:10 p.m.). These times correspond to time (in hours) of zero in subsequent discussion. Also, the temperature cycles in earlier days were similar. An infrared thermometer (RadioShack, Fort Worth, Texas, USA: #22–325) was used to measure the wall temperature, and a digital thermometer (RadioShack, Fort Worth, Texas, USA: #63–1035) displayed the inside and outside air temperatures. The air and wall temperature readings were taken at a height of approximately one meter. Both thermometers have an error of approximately 0.4°C.

It is important to note here that ceiling and floor temperature measurements were not obtained in this work. Also, the temperature measurements were obtained under conditions that did not permit skylight or earth tunnel operation.

Results

Temperature measurements

The three temperature profiles shown in Fig. 5 illustrate the effect of orientation on each room's climate. The northern room and the northwestern room experience an internal air temperature fluctuation of only four degrees, while the southern room experiences a 5° variation throughout the day. The maximum temperature achieved in each room seems to be dependent on the orientation: the north and northwest rooms reach maximums of 31 and 32°, respectively, and the southern room reaches a maximum of 33 °C. However, the northwestern and southern rooms exhibit nearly identical average temperatures, 0.5° higher than the north-facing room. This seems to indicate that while maximum temperature is a function of orientation, while the average temperature may be more closely linked to architectural variations between the rooms, such as ceiling differences.

Heat transfer calculations

The heat transfer calculations focus on the interior of the structure, giving insight into the heat flowing between the air and inside wall surface of each room. Based on these calculations, in conjunction with the rate of temperature increase within each room, the role of the remaining surfaces (other walls and ceiling, for example) can be assessed. The data indicates that the outer wall plays a distinctly different role in each of the three rooms. Figure 6 shows that the temperature differential that drives the interior heat

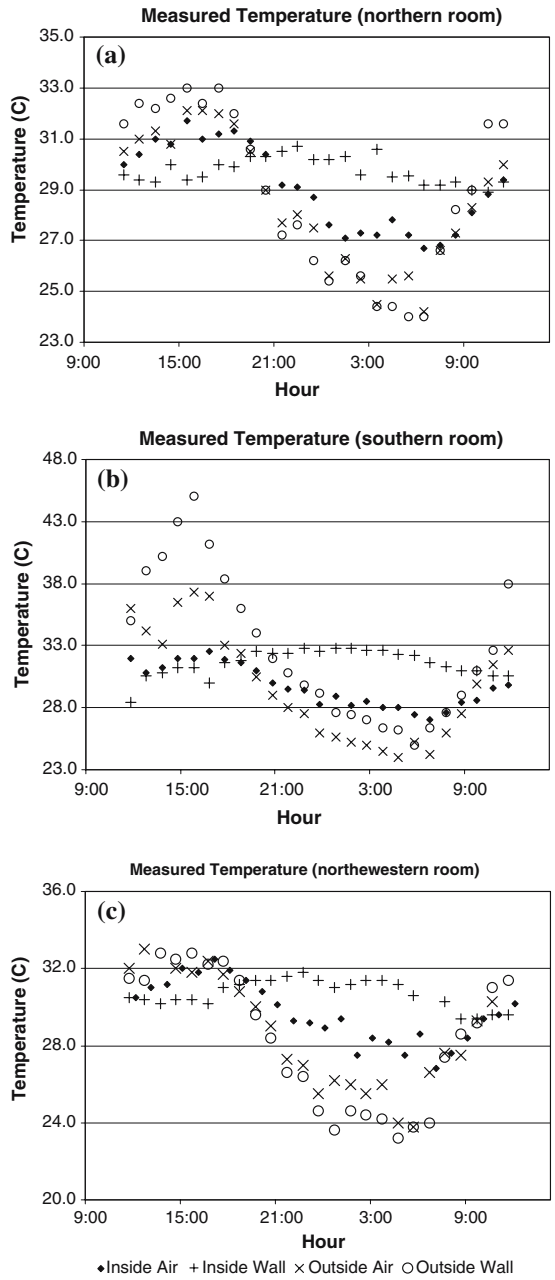

Fig. 5 Measured temperature profiles for the three rooms

transfer (between the inside air and the inner wall surface). This takes a different form for each of the three rooms, leading to dramatically different behavior for each wall. In the north-facing room (see Ref. 2 and Appendix A for a description of each room), the temperature differential curve is nearly evenly distributed between a positive and negative value. This leads to zero net heat transfer (within the calculated error) through the wall throughout the day (see Fig. 7). Note that the abscissa corresponds to time in hours after starting the measurements.

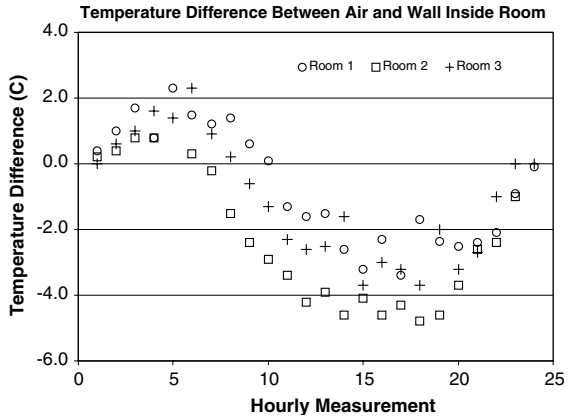

Fig. 6 Temperature differential between air and wall in each room

The temperature differential curve for the northwest room takes a slightly more negative net value on Fig. 7. This is due to the presence of solar radiation in the evening on the western façade. Consequently, there is a net amount of heat transferred into the room from the wall (a negative amount of heat transferred from the inside air to the wall). In the southern room, the temperature differential takes a negative value for much of the day. As a result, the southern wall is a source of heat on a net basis (see Fig. 7). In room 2—the southern room—a second wall was monitored as well. This second wall, built between the room and a courtyard also provides heat to the room on a net basis. It is important to note here that the ranges of heat fluxes presented in Fig. 7 correspond, respectively, to the maximum and minimum temperatures measured within the 24 h periods of the measurements.

Based on the air temperature profiles and room geometries, it was possible to calculate the heat flowing into each room throughout the day (the heat required to cause the observed temperature fluctuation). Due to the discrete nature of the temperature measurements, it became necessary to smooth the small amount of scatter by fitting a sinusoidal equation to the data. This ensures that the heat flow is calculated from the macroscopic temperature gradient rather than small-scale measurement error. The total heat flow was compared to the heat passing through the wall(s) in order to determine the role of the remaining surfaces within the room (the ceiling, in particular). The results are shown in Fig. 8. As in Fig. 7, the ranges in the heat flow data correspond to the measurement maximum and minimum temperatures.

For the northern room, in which there is no net heat transfer through the outer wall, the remaining surfaces exhibit no net heat flux, within error. Beyond examining the net value of the heat transfer, it is interesting to note the shape of the curve. Figure 8 compares the heat flow with a scaled outside temperature curve. The abscissa corresponds

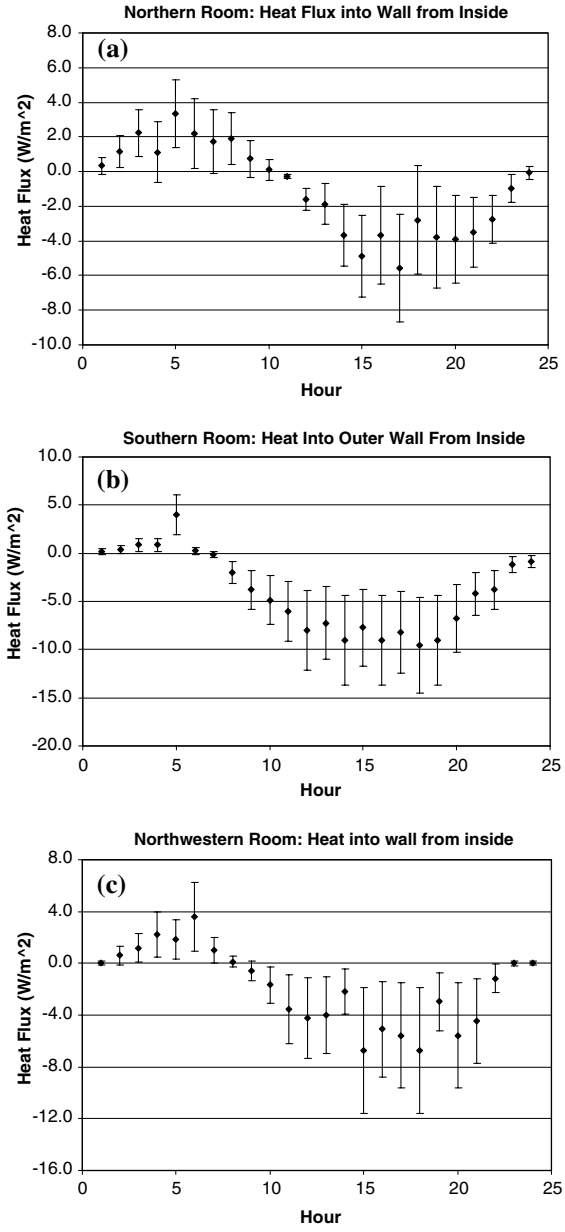

Fig. 7 Heat transfer occurring through each wall

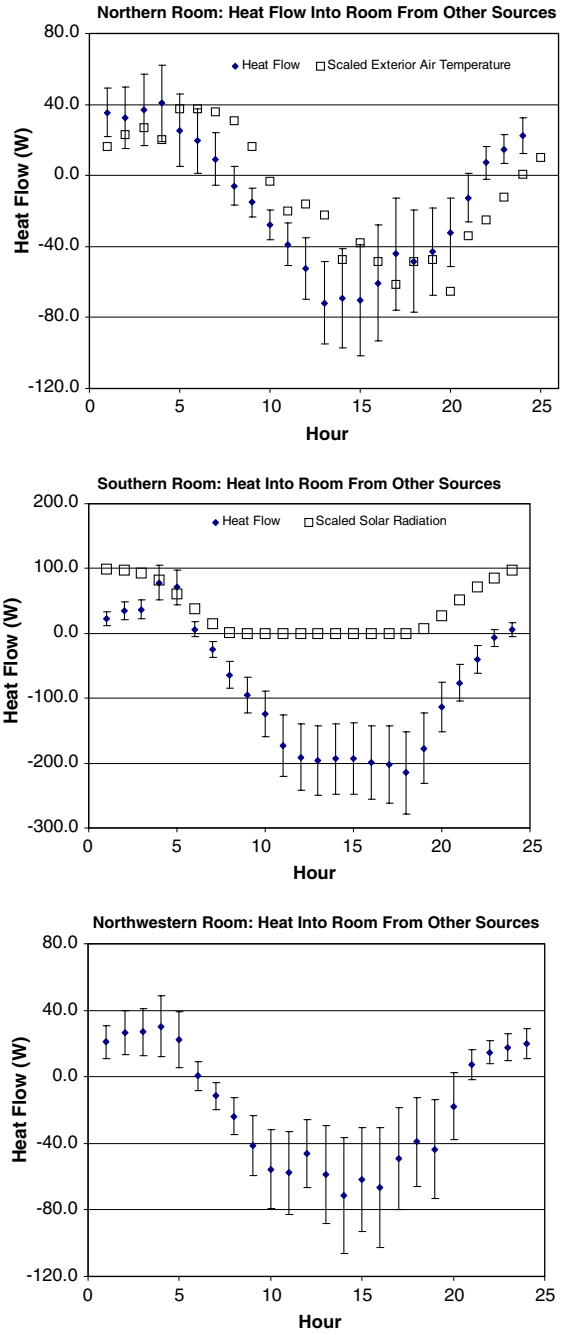

Fig. 8 Heat entering each room from other sources

to time in hours after starting the measurements. It appears that the driving force behind the heat transfer behavior of the northern room is the exterior ambient temperature.

In contrast, the southern room does experience a significant amount of heat influx through its outside wall. Figure 8 shows the heat that must be entering into the room from other surfaces in order to account for the inside air temperature profile. The shape of this heat flux curve is very different from that seen in the northern room; the outside temperature alone does not account for the calculated heat flow. Rather, the driving force in the case of the southern room appears to be the solar radiation incident upon the building, displayed in Fig. 8. Although it was not possible to record the solar flux on the day the temperature measurements were taken, solar data from a comparable day was used. The data was recorded in 1998 at the Inshas facility, and also in July.

As discussed above, the northwestern room experiences a small net heat flux into the room through the northern wall. As a result, there must be a net heat flux out through the other surfaces of the room over the course of the day. The heat flux through these other surfaces is seen in Fig. 8. Interestingly, the behavior of the heat flux through other

surfaces in the northwestern room appears to be a compromise between the northern and southern rooms. Indeed, this is expected, as the northwestern room receives some solar radiation due to its western façade, but is still heavily controlled by the exterior air temperature.

Discussion

Model validation

The theoretical model presented in Sect. ''Theoretical model and computer simulation'' predicts that the time lag and decrement factor seen across a wall are only functions of wall thickness and thermal diffusivity, as shown in Fig. 3. The temperature measurements taken at the Inshas facility offer an opportunity to test this model. Using the data presented in Table 1, it is possible to calculate the decrement factor and time lag of the inner wall surface with respect to the outer surface for each room (the time lag calculations are normalized by 24 h). The results obtained arbitrarily for the three walls, plotted in Fig. 9, indicate that all three walls have a very similar ratio of thickness squared to thermal diffusivity. In fact, the three walls have identical thickness and material composition. This indicates that the time lag and decrement factor are dependent on wall thickness and diffusivity, and are not functions of orientation, heat flux, or temperature variation.

To assess the validity of the computer simulation, the theoretical time lag and decrement factors were compared to those generated by the computer program for a wide range of wall thickness, diffusivity, and thermal loading conditions (Figs. 10, 11, respectively). The simulation shows that time lag and amplitude reduction are not dependent on imposed boundary conditions (solar radiation, for example). Each data point represents a unique simulated scenario; wall thickness, diffusivity, room size, and heat loading were varied methodically to generate the data. In the case of time lag, the simulation agrees very well with the theoretical prediction. Similarly, the simulated decrement factor follows the same trend as the theoretical model, but the agreement is not as strong as for the time lag.

The widespread agreement between theoretical, computational, and experimental results shows the initial success of the study. However, much work is required before the passive solar concept can be effectively applied on a global scale. The relationship between ceiling design and heat transfer requires further study; the effect of composite materials on thermal properties is certainly important, and

Table 1 Measured temperature parameters

		Mean Value 0.1	Amplitude (Peak to Peak)	Time lag relative to outside ambient (h)
Outside	Ambient	28.9	10	N/A
Room 1	Outside Wall	28.8	9	0
	Inside Wall	29.5	1	7
	Inside Air	29.1	4	0
Room 2	Outside Wall	32.7	20	0
	Inside Wall	31.6	3	10
	Inside Air	29.6	5	1
Room 3	Outside Wall	28.3	8.5	0
	Inside Wall	30.7	1.5	7
	Inside Air	29.7	4	1

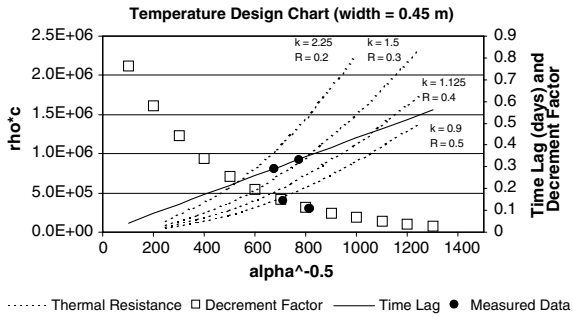

Fig. 9 Temperature design chart showing measured phase lag and amplitude reduction

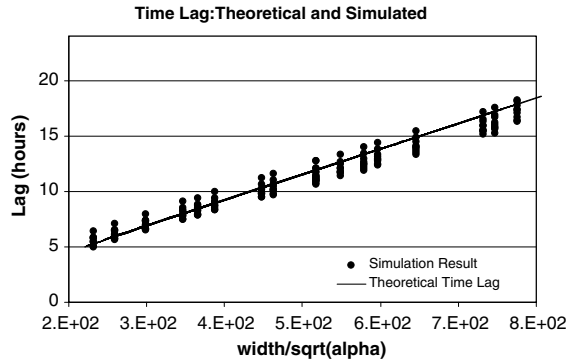

Fig. 10 Comparison of theoretical and simulated time lag

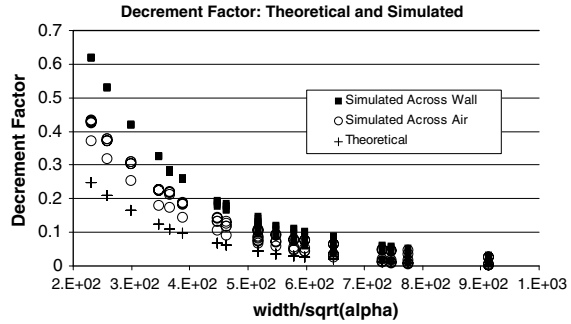

Fig. 11 Comparison of theoretical and simulated decrement factor

the behavior of buildings operating under normal conditions (with windows and doors open to encourage natural ventilation) must be investigated.

Design considerations

To provide for optimal thermal comfort, the designer must choose a material with a balance of thermal properties in addition to an appropriate wall thickness to match the material choice. In particular, the need to control time lag and thermal amplitude inside a room leads the designer to a certain material, based on thermal diffusivity (as shown in Fig. 3). However, the designer must remember that the mean temperature shift is dependent on thermal conductivity rather than diffusivity. Therefore, a balance of thermal properties is needed in order to achieve all-around thermal comfort.

Also, the design of a passive solar building must include the coupling of other walls, the ceiling, and interior heat sources, such as appliances. A preliminary approach to this issue is presented in Eqs. 11 and 12 of Sect. ''Thermal resistance as a design tool''. This study indicates that the ceiling likely plays a critical role in the establishment of thermal comfort in passive solar structures. Therefore, the integration of materials selection and architecture is especially important when designing the ceiling.

Of course, a crucial consideration in the design process is cost. As presented in Sect. ''Cost model'', the cost of providing optimal thermal performance is dependent on the material selection. Figure 12 shows a graphical representation of the cost of various materials. Materials closest to the origin of the plot are the most cost-effective based on the theoretical analysis; cement and concrete are identified as optimal building materials. Sandstone, marble, and brick also have a relatively low cost. However, it is important to consider the life cycle cost of a structure when making architectural and materials decisions. For example, if a given material is capable of significantly reducing energy costs during the lifetime of the building, then the initial expense of the material may be justified.

Implications

The implications of the current work are quite significant. First, the agreement between the experiments and theoretical results clearly shows that the simple heat diffusion concept captures the essential physics that controls the wall and air temperatures. Hence, the merit indices derived for thermal performance and cost may be used to guide the selection of the most appropriate materials for affordable housing that are cooled or heated using passive solar concepts.

In the case of passive solar heating, the key idea is to store the heat in the walls during the peak hours of sunlight (this also provides internal cooling as long as the external heat does not diffuse completely to the inner walls). The heat is then transmitted into the building once it reaches the inner wall, presumably at night when it is cooler. The heat diffusion can be controlled through the integration of architecture and material selection, and hence the times for heating and cooling.

Before closing, it is important to discuss the issue of cost. As a first step, the current paper considers the cost per unit area, and uses this in the extraction of a cost merit index (Section ''Cost model''). Based on this, the best materials for use in passive solar heating are cement, concrete, stone, and brick (Fig. 12).

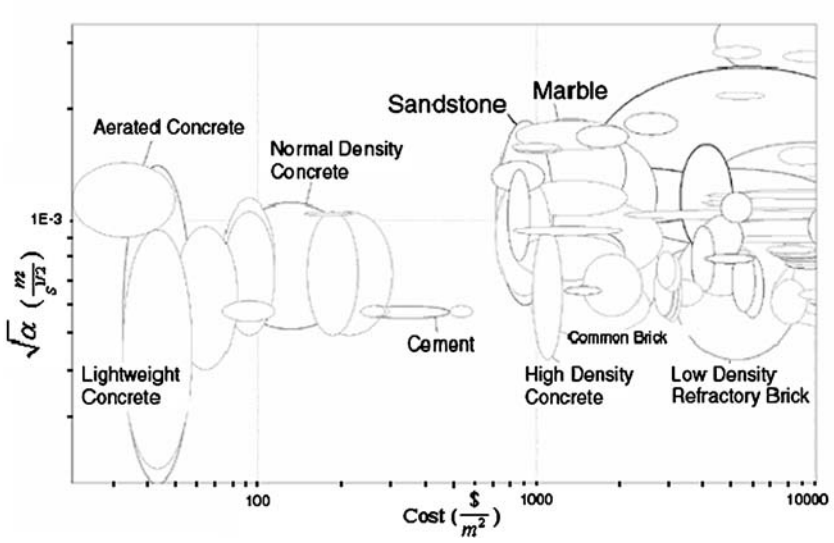

Fig. 12 Cost analysis

However, the above cost model does not consider the life cycle cost reduction associated with diminished energy costs for heating and cooling over the life of the home. These will clearly vary from place to place. Nevertheless, such costs must be estimated per unit increase in diffusion length or wall thickness. In this way thermal performance can be balanced against life cycle costs associated with increased wall thickness or new affordable building materials. This is clearly a challenge for future work.

Furthermore, in assessing the life cycle cost, it will be important to subtract the savings in heating, ventilation and air-conditioning (HVAC) costs due to the use of passive solar approaches, must be adjusted by the incremental cost of the thermal mass that is needed to achieve the desired thermal conditions. Such calculations require information and analyses that are beyond the scope of the current paper. Nevertheless, it is important to note here that such life cycle analyses are likely to favor low cost building materials, since the incremental cost of thermal mass must be less than the life cycle savings in HVAC costs for the proposed passive solar approaches to be attractive.

Finally, it is important to note here that the convection heat transfer between the inner air and the walls or ceilings is critical to maintaining comfortable internal temperatures. This can be achieved by cross-ventilation, the use of holes in the ceilings, and dome architecture that provides a natural boundary layer of air that facilitates convective heat transfer from the inside of the building into the walls. These effects remain as interesting challenges for future work.

Summary and concluding remarks

This paper presents the results of a combined experimental, theoretical, and computational study of materials selection and design for thermal comfort in passive solar buildings. The salient conclusions arising from this study are as follows:

1. A balance of thermal properties is needed to maintain thermal comfort inside of a building. While time lag and amplitude reduction are dependent on thermal diffusivity, the mean temperature shift is a function of thermal conductivity. A temperature design chart is presented displays the influence of materials selection on thermal comfort.
2. The simple one-dimensional heat diffusion theory used to model time lag and decrement factor agrees with the measurements taken at the Inshas Guest House as well as the data generated by the computer simulation. The time lag and decrement factor are shown to be only functions of wall thickness and thermal diffusivity.
3. The orientation of a room strongly influences the heat passing through the outer walls. In the case of the northern room, the exterior wall is seen to be totally passive, in that it does not provide or remove a net amount of heat to the room during a 24-h period (heat is removed from the room during the day and provided during the night). The heat transfer is seen to be primarily driven by the exterior air temperature. In contrast, the southern wall is a large source of heat for the room—mainly during the night—and is seen to be influenced largely by the direct solar radiation incident upon the exterior wall surface.

Acknowledgements The authors are grateful for financial support provided by the NSF Division of Materials Research. Appreciation is extended to the Program Manager, Dr. Carmen Huber, for her encouragement and support. This paper is dedicated to the memory of the late Prof. Fawzy Hammad.

Appendix

Appendix A: Inshas Facility Description

The Inshas Science City project was established by the Egyptian Atomic Energy Authority in 1991. This project is located at the Inshas research center, about 35 km from Cairo. The project was erected to demonstrate a new approach for sustainable desert architecture in Egypt. The aim is not only to revive traditional desert Egyptian architecture, but also to incorporate new sustainable approach for desert architecture.

The Guest House Building (Fig. 13) was designed to accommodate scientists and visitors to the Inshas Research Center. The building has a total area of 2500 m^2. It contains eight mini-apartments, each with two double bedrooms, common bathroom and kitchenette, and six single bedrooms with the same facilities. It also includes a large dining hall (multi-purpose hall) with kitchen area and administration offices. The load bearing masonry walls were constructed with quarried limestone blocks ($40 \times 20 \times 20$ cm), while the roofs comprise vaults and domes made from burnt bricks ($25 \times 12 \times 6$ cm). Temperature measurements were obtained from the north, south and northwestern rooms shown in Fig. 13.

The north room is a bedroom located at the north side of the building. It has a square ground plan and a hemispherical dome roof with skylight on the top of the dome. The room has a height of 4.5 m and it occupies an area of 3.5 m × 3.5 m. The 40 cm thick walls are covered with 2 cm of cement mortar. The room has a domed roof that is 25 cm thick. The south room is an office with a rectangular area (3.5 m × 5.5 m) and a height of 5.3 m. The limestone walls are 40 cm thick, and covered with 2 cm of cement

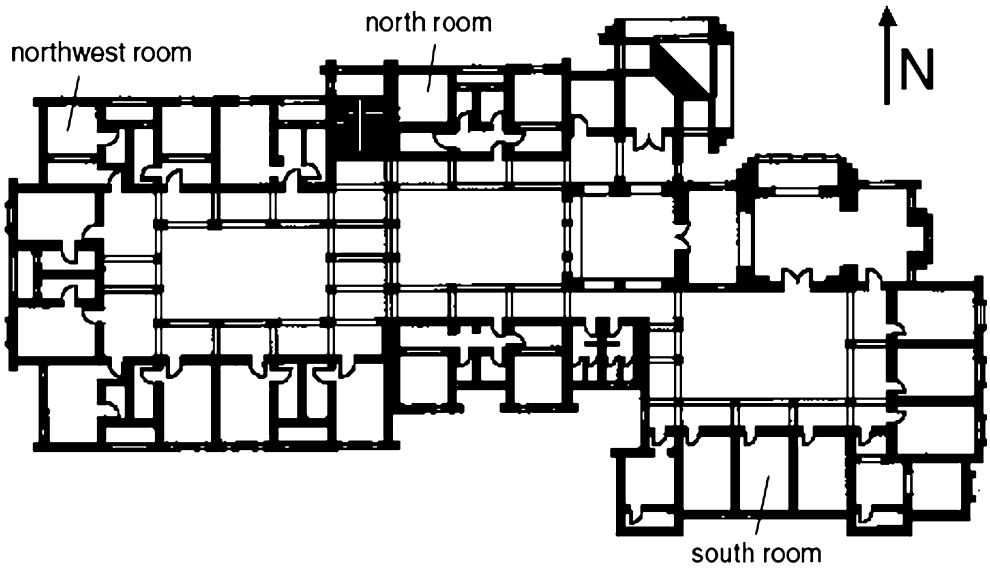

Fig. 13 Plan of guest house building

mortar and interior paint. The room has a barrel-vault roof with 25 cm of burnt brick.

Finally, the northwest room is a bedroom on the first floor on the northwest corner of the building. It has a square floor area (3.5 m × 3.5 m) and a height of 3.5 m. The 40 cm thick limestone walls are covered with cement mortar and paint. The room has a dome roof that is constructed from 25 cm thick brick.

References

1. Fathy H (1973) Architecture for the poor: an experiment in rural Egypt. University of Chicago Press, Chicago IL
2. New Technologies for Desert Development: The Inshas Science City Project (1997) Forschungszentrum Jülich and Egyptian Atomic Energy Authority, Germany
3. Bansal N, Hauser G, Minke G (1994) Passive building design. Elsevier Science B.V., Netherlands
4. Givoni B (1976) Man, climate, and architecture, 2nd edn. Applied Science Publishers, Ltd, Essex, Britain
5. Ashby MF (1999) Material selection in mechanical design. Butterworth-Heinemann, Burlington MA
6. Holman JP (2002) Heat Transfer, 9th edn. McGraw Hill, New York NY